TECHNICAL MEMORANDUMS

NATIONAL ADVISORY COMMITTEE FOR AERONAUTICS

No. 756

THE BEHAVIOR UNDER SHEARING STRESS OF DURALUMIN STRIP WITH ROUND, FLANGED HOLES

By Karl Schüssler

Luftfahrtforschung
Vol. 11, No. 3, August 18, 1934
Verlag von R. Oldenbourg, München und Berlin

Washington
October 1934

NATIONAL ADVISORY COMMITTEE FOR AERONAUTICS

TECHNICAL MEMORANDUM NO. 756

THE BEHAVIOR UNDER SHEARING STRESS OF DURALUMIN STRIP WITH ROUND, FLANGED HOLES*

By Karl Schüssler

SUMMARY

This report presents the results of an investigation to determine the behavior of duralumin strip with flanged holes in the center when subjected to shear stresses. They buckle under a certain load just as a flat sheet. There is one optimum hole spacing a_o (equation 4) and one corresponding buckling load in shear p_{ko} (equation 7) for each sheet width, sheet thickness, and flange form. Comparison with nonflanged sheets revealed a marked increase of buckling load in shear due to the flanging and a slightly greater displacement. The stiffening effect of flanging showed itself in a considerably higher buckling load for thin, wide strip than for the unweakened sheet. Lastly, the displacement δ, under a 1 kg/mm (55.99 lb./in.) load (equation 8) was determined. It is considerably higher for the flanged sheet than for the unweakened sheet, and slightly higher than for the unflanged sheet. Sheets may not be stressed beyond buckling load unless special cross stiffeners are available to take up the load component K perpendicular to the direction of shear. The shear-displacement diagram (fig. 6) is substantially a tensile stress-strain diagram above the buckling load. The formulas developed for a_o, p_{ko}, and δ are the results of pure experimentation and may therefore become quite faulty outside of the analyzed range.

---

*"Uber das Verhalten von Leichtmetallblechstreifen mit kreisrunden, randgebördelten Löchern bei Schubbeanspruchung." Luftfahrtforschung, August 18, 1934, pp. 74-85.

INTRODUCTION

A very popular structural member in light-metal airplane and airship design is the flat, thin metal strip with lightening holes, the edges of which are generally flanged for reasons of stiffness.

The loads are, as a rule, not taken up by the individual sheet since it forms, with other sheets, corrugated sheets, rods, or angles, an elastic structure: such as of a spar, compound spar of two or more spars, float frame, airship girder, etc.

The location of the forces relative to the elastic axis of the system is essential for the type of stress. The forces lying on a plane with this axis simply set up tension, compression, or bending in the elastic structure, whereas all others effect an additive torsion. This stresses, apart from specific cases, the individual sheets in shear. When the forces are at great distance from the elastic axis, the shear may become so great as to make the other stresses negligible; that is, make it a case of simple shearing stress.

NOTATION

a	mm,	hole spacing.
a_o	"	optimum hole spacing.
b	"	width of sheet.
d	"	diameter of hole.
D	"	diameter of flanging.
E	kg/mm²,	Young's modulus.
G	kg/mm²,	modulus of shear.
L	mm	length of sheet.
p	kg/mm,	shearing stress.
p_k	"	buckling load in shear.

(kg/mm² × 1422.35 = lb./sq.in.) (mm × 0.03937 = in.)

p_{ko}	kg/mm,	p_k value of a_o.
p_{ku}	"	p_k value for smooth sheet.
P	kg,	shearing force.
r	mm,	distance of last hole from edge.
s	"	thickness of sheet.
v	"	displacement.
v_k	"	displacement during buckling.
δ	$\frac{mm}{kg}$,	displacement for P = 1 kg (2.20462 lb.).
δ_1	mm $\frac{mm}{kg}$,	relative displacement for p = 1 kg/mm.
μ,		10^{-3} mm.

PREVIOUS SHEAR INVESTIGATIONS ON METAL STRIP

The behavior of infinitely long, flat strip in shear is determined by calculation and the calculation is checked by experiment. The sheet remains flat at first and the displacement v is proportional to the shear load p:

$$v = \frac{p}{G}\frac{b}{s}$$

where b = width, s = gage of sheet, and G = shear modulus of the structural material.

Upon reaching a certain shear load uniform corrugations or waves are formed which at first run at about 45° in the direction of shear, and v, rather than remaining proportional to p, now increases; the sheet buckles (fig. 1).

Bryan, Lilly, Timoschenko, and Ritz (references 1 to 5) have developed approximations for computing the buckling stress in shear and the spacing of the wrinkles λ, while Southwell and Skan (reference 6) found the rigorous mathematical solution. As with the compression member, it results in an infinite series of load values at which the flat sheet stressed in shear is unstable; that is, buckles. The lowest and therefore decisive value is:

$$p_{ku} = \frac{88.7 \ E \ s^3}{12\left[1 - \left(\frac{1}{m}\right)^2\right] b^2} \tag{2}$$

where E = Young's modulus and m = Poisson's ratio of the material. The corresponding wave length is:

$$\lambda = 1.6 \ b \tag{2a}$$

These mathematical results were checked against buckling in shear experiments. With shear distributed uniformly along whole sheet length L, the shear force P and L give $p = \frac{P}{L}$ or, if two identical sheets are stressed concurrently,

$$p = \frac{P}{2L} \tag{3a}$$

But with finite sheet length p must drop to zero at the free ends; that is, it cannot be constant across L. The last elements at the free ends cannot transmit the shear forces to adjacent elements; i.e., they must be shear free.

According to Coker's experiments below the buckling limit (reference 7), sheets which are very long in comparison with their width manifest a shear load p, which is practically constant across the whole length and only drop on a short piece at the edge. In approximation we may assume $p = 0$ on two end strips of length $b/4$ and constant on the intermediate piece of length $L - 2\frac{b}{4} = L - 0.5 \ b$. This gives $p = \frac{P}{L - 0.5 \ b}$, or for two identical sheets:

$$p = \frac{P}{2L - b} \tag{3b}$$

The buckling tests in shear made by Bollenrath (reference 8) gave a buckling load in shear of about 43 percent according to (3a), and of about 37 percent, according to (3b) below the theoretical value computed according to (2). Even the wave length varied from the theoretical value $\lambda = 1.6 \ b$ (2a), averaging 1.94 b.

Mathar (reference 9) explained these discrepancies as follows: The shear force is not evenly distributed over the whole length of the clamping strips, but introduced only at one or two places. The elastic strips must take up the shear forces and become elongated. The displacement and through it the shear load p is, as a result, higher at the points contiguous to the applied load than farther away. On the other hand, buckling is contingent upon the maximum value of p, because as soon as p exceeds p_{ku} (equation 2) at any place, buckling must occur. Owing to favorable, i.e., relatively rigid fixation, Mathar obtained buckling figures which are only 5 percent below p_{ku}, and a wave spacing of 1.6 b, that is, corresponding to the theoretical figure (equation 2a).

Seydel (reference 10) analyzed flat, rectangular plates with stiffeners parallel to the edges and adduced an example of transversely riveted angle stiffeners.

Schmieden (reference 11) computed very thin, infinitely long sheets with superposed, closely spaced small cross stiffeners, to which longitudinal stiffeners may be added. The mathematical accuracy of his formulas is dependent upon all very small quantities becoming infinitely small.

Bergmann and Reissner (reference 12) approximated corrugated sheets with corrugations parallel or perpendicular to the direction of shear as flat plates with varying bending stiffness in the two mutually perpendicular directions.

Jennissen (reference 13) experimented on corrugated plates divided by brackets in separate panels. He developed an approximative method for their calculation and obtained a close agreement between experiment and theory. The problem of sheets weakened by holes has equally been attacked.

Hirota (reference 14) calculated the stress attitude prior to buckling in an infinitely long metal strip with a hole in the center when stressed in shear.

Mathar (reference 9) determined experimentally the buckling load of strip with round holes evenly spaced over the center line. He found that holes of d = 70 spaced a = 140 mm, reduced the buckling load in a duralumin strip (s = 0.7 mm, b = 110 mm) by about 50 percent while raising v by nearly 110 percent.

The present experiments were primarily intended to ascertain whether it would be possible to stiffen a sheet weakened by holes with flanging the holes' edges enough to assure a buckling load p_k approaching or even exceeding the buckling value of the unweakened strip p_{ku} (equation 2).

EXPERIMENTAL SET-UP

The experimental arrangement is that developed from Mathar's and Jennissen's tests. It is shown in figure 2.

Two identical strips are clamped between two stationary end rails and one sliding center rail at which the shear is applied. Naturally the fixed spacing of the side rails produces minor additive tension perpendicular to the direction of shear with the displacement which, however, may be disregarded with respect to the shearing stresses; with α = angle of displacement the width b should diminish to $b \cos \alpha$. As α remained consistently below $0^\circ 20'$ up to buckling, the additive tensile stress could at the most reach $(1 - \cos 0^\circ 20')$ E; that is, $(1 - 0.99997) \times 7{,}500 = 0.225$ kg/mm², while in general it amounted to only a fraction of this figure because α is mostly considerably lower.

The force was measured with a tension stirrup up to 20 t (point 1, fig. 2) and a compression dynamometer up to 10 t for high loads in isolated tests (point 2, fig. 2). The possible error for the tensiometer was ±8 kg. As P_k, the buckling load in shear, is $\geqq 500$ kg in all tests, this error amounts to $\leqq \frac{8}{500}$, that is $\leqq 1.6$ percent.

With compression gage added, the possible error is ± 7 kg higher for instrument friction and error in reading as well as +19 kg for each 1° C. temperature rise caused by the expansion of the mercury in the dynamometer. Without temperature correction this error is below ±38 kg corresponding to 2° C., with correction ±9.5 kg or equivalent to 0.5° C. temperature error in the pressure recorder. The total instrumental error is therefore 7 + 38 = 45 kg in the first, and 7 + 9.5 = 16.5 kg in the second case. The total error in shear is under the most adverse conditions, 8 + 45 = 53 kg without, and 8 + 16.5 = 24.5 kg with temperature correction. Compared to only 8 kg without compression gage, these errors are high, for which reason the measurements were as a whole made only with the tensiometer.

(t (ton) × 2204.62 = lb.)

The displacement was recorded with the Zeiss dial gage (point 3, fig. 2). As a check, we used the Martens mirror instrument in some tests (points 4a and 4b in fig. 2). The dial gage admits of an error in reading of 0.001 mm. The displacement at the point of collapse v_k was always $\geqq$ 0.074 mm, so the percentage of error was always $\leqq \frac{0.001}{0.074} = 1.4$ percent.

The error due to elongation of the center rail which transmits the shearing force is also small. Working with the tensiometer alone (most unfavorable case) and assuming p to be constant over the whole length L, the force to be transmitted by the center rail from the beginning to the end of the strip drops linearly from P to zero; it averages $0.5\ P$. The corresponding mean stress is $\sigma_m = \frac{0.5\ P}{F} = \frac{0.5\ P}{2\ B\ H}$, where B and H represent the width and height of the upper and lower half of the center rail. Owing to this stress the rails have a total elongation of $\delta = \frac{\sigma_m\ L}{E} = \frac{0.5\ P\ L}{2\ B\ H\ E}$. With a displacement v for a pertinent P, the relative discrepancy in displacement and consequently that of its proportional shear load p amounts at the most to:

$$\frac{\delta}{v} = \frac{0.5\ P\ L}{2\ B\ H\ E\ v} = \frac{0.5\ L}{2\ B\ H\ E}\ \frac{P}{v}\ .$$

$\frac{P}{v}$ is maximum for strip 33: $P_k = 3{,}000$ kg; $v_k = 0.162$ mm. Therefore,

$$\frac{\delta}{v} = \frac{0.5 \times 1192}{2 \times 160 \times 32 \times 21000} \times \frac{3000}{0.162} = 0.051 = 5.1 \text{ percent.}$$

This discrepancy between maximum and minimum p corresponds to a difference of about ±3 percent from the mean value.

In the most unfavorable case the total error equals the sum of the individual quotas:

$$f_{total} \leqq 1.6 + 1.4 + 3 = 6 \text{ percent.}$$

The buckling was also determined separately from the wrinkles which caused the image of a cross in the sheet to become distorted.

GENERAL RESULT OF BUCKLING TESTS

The samples were duralumin 681b of the Düren Metallwerke, in strips of 2500 X 500 mm length and of 0.4, 0.5, 0.6, and 0.8 mm thickness. Its Young's modulus was $E = 7,500$ kg/mm^2, with a shear modulus of $G = 2,900$ kg/mm^2.

Aside from several flat strips and one perforated strip without flanging, the rest all had flanged holes - each pair of strips having the same hole diameter, spacing, and type of flanging.

The flanging was beveled. The form is shown in figures 3 and 4 along with the male and female dies. The bevel angle was made the same as the friction angle with grease lubrication to allow smooth removal of the male die after flanging operation.

The preparation of the samples was effected with great care. They were cut out to the correct length and width and, if necessary straightened. The holes were drilled to 1/10 diameter (centering hole) and then cut out with a cutting tool. The flanging operation consisted of pushing with male and female dies (fig. 4).

We investigated the effect of:

1. Strip width, b.

2. Strip thickness, s.

3. Diameter of flanging, D.

4. Depth of flanging. This may be changed for given flanging form by means of the cut-out hole diameter, d: flanging depth $\cong 0.5\ (D - d)$.

5. Hole distance, a.

The flanged strip behaved the same as the flat strip under shearing stress. Up to a certain load stage, the strip remained flat, the shearing force P is proportional to the displacement v. The distance of the wrinkles equals the hole spacing a. The test points deviate simultaneously from the previous straight line and follow a new straight line after a few points (fig. 6). The center of the two straights was taken as the buckling point of the strip. With further stress the curve deviates from the straight line because the yield point is soon exceeded as a result of the great deformation of the buckled strip. Figure 7 shows a curve with several unloadings. This graph is valid only for constant strip width b under load as in the present experiments. The shearing force S before buckling (fig. 8, left) assumed divided in tension Z and compression D consists, after the strip buckled with respect to compression D (fig. 8, right of D which, analogous to the buckled compression member, remains practically constant), of tension Z and a new component K perpendicular to the direction of shear. Z and K grow in the same proportions as S. In relation with Z and therefore S the extension of the visualized tension members and through them the displacement v, is proportional to the elongation due to Z. Figure 7 is therefore essentially a stress-strain diagram. The K component in the present experiments is taken up by the clamping rails. In practical cases, however, a stress above the buckling limit is possible only when there are special cross stiffeners to take up K. In simple strips the two longitudinal edges come consistently closer together because of K; the strip is destroyed in the present experiments through tearing of the flanged edges. Figure 9 shows a severely deformed, torn strip. The deformation, considerably magnified, is the same as immediately after buckling (fig. 5).

The majority of tests was made with strip lengths of $L \cong 1,192$ mm. The buckling force in shear of the flanged strip P_k should be assumed proportional to the strip length, as shown in figure 10. The buckling load in shear p_k is defined from the buckling force in shear P_k and strip length L according to (3a):

$$p_k = \frac{P_k}{2L} \tag{3}$$

The figures in figure 10 are those of table I for strip 17 to 19, 41 to 45, and 47. The displacement in buckling v_k (in mm) is for identical sheets of varying length, naturally always the same, because the sheet consists of identical strips of length a which, regardless of their number, are identically distorted.

The effect of the flange depth is subordinate as seen from table I, sheets Nos. 43 to 45. P_k remains constant within wide limits with increasing d, that is, decreasing flange depth 0.5 (D - d), while v_k shows a slight increase for smaller flange depth. The explanation for this behavior is that for deflection perpendicular to the plane of the sheet, that is, for buckling, the flanged hole should be considered as rigid relative to the sheet, as soon as the flanging has reached a certain minimum depth. By the same argument, not the flanged hole but rather the part of the sheet which remained flat, is the decisive factor for the buckling load since it remains the same in any case when d is changed. On the other hand, the flanging is more readily bent in the direction of the plane of the sheet than the unweakened, flat part of the sheet. Consequently, a deeper - that is, stronger - flanging assures less displacement for identical load. P_k is essentially more important for the designer than v_k. But any improvement in the flanging can only involve an improvement of v_k, not of P_k, because P_k is governed by the flat part of the sheet. In general, the form of flanging is therefore subordinate when it has a certain minimum stiffness perpendicular to the plane of the sheet only with given D. Logically, D only needed to be changed, but not d.

The flanging operation increases the perimeter of the hole from πd to πD, and it is necessary to assure that the resulting unit elongation $\frac{\pi (D - d)}{\pi d} = \left(\frac{D}{d} - 1\right)$ does not exceed the ultimate, because the edges would tear otherwise. Small irregularities on the edge of the hole act as notches very favorable for tearing. With smoothly cut holes flange tearing can be safely avoided in the kind of material and the shape of flanging used here when $d \geq 0.85 D$.

Figure 11 shows the effect of hole spacing a versus buckling load P_k. The curves have a distinct maximum for comparatively small a, which lies above or below the shear load in buckling of the unweakened sheet $P_{ku} = p_{ku} (2L - b)$. (Compare equations (2) and (3b).) The maximum is due to the fact that the flanging as already pointed out is rigid in bending perpendicular to the plane of the sheet as compared to the unweakened sheet, while being more easily deformable in direction of the plane of the sheet than the unweakened sheet; i.e., takes up practically no shearing stress. The greater the number of flanged holes in a sheet, the greater is the number of bending resistant circular surfaces of diameter D; the higher is the value at which the sheet wrinkles perpendicular to its plane. On the other hand, the sheet which, after all, is supporting only in the flat portion, is so much higher stressed as there are holes. Both effects are contrariwise, hence the maximum.

The behavior with wide-hole spacing a was not investigated. With very high a values, that is, few holes, the p_k value should approach the buckling value of the flat sheet without holes p_{ku} (equation 2). Other extreme values may appear between these limits, but they are not very important because the holes must, for reasons of weight saving, be spaced as closely as possible. In the following, no importance therefore was attached to the maximum other than for small a. All values valid for this maximum carry the subscript o.

OPTIMUM HOLE SPACING a_o

The first significant question is, the best hole spacing a_o at which the maximum occurs for a given sheet thickness s, width b, and diameter D. It is not necessary to define a_o very accurately because the contiguous P_k values do not vary appreciably from P_{k_o} maximum when a deviates a little from a_o, owing to the horizontal tangent of the curves $P_k = f(a)$.

The effect of b on a_o was so little in the analyzed range as to escape definition. The reason for this is that the center strip of the sheet governs the buckling. But this strip naturally has always the same aspect for otherwise identical sheets of different width.

The relationship between a_o and s is parabolic, according to table II and figure 12: $a_o = \alpha \quad s$ a_o increases considerably with increasing s for thin sheets, less for thicker sheet. The reason for this is that the bending stiffness of the sheet rises perpendicularly to its plane with s , while the stiffness of the flanging increases only with s. Admittedly, the stiffening effect of the flanging is not as great for thicker sheets which of themselves are already very stiff, so that the holes must be spaced farther apart than in thinner sheets. The explanation for the smaller rise of the curve of thicker sheets is that, for example, a 0.1 mm thickness change means comparatively less in a thick than in a thin sheet.

The factor α varies in linear relation with D (table II and fig. 13): $\alpha = 68.5 + 0.8\ D$. Consequently,

$$a_o = \alpha\sqrt{s} = (68.5 + 0.8\ D)\sqrt{s}$$

$$a_o = 0.8\ (D + 86)\sqrt{s} \tag{4}$$

Far outside of the investigated range: $D = 62$ to 82, $s = 0.4$ to 0.8 mm, $b = 75$ to 215 mm, the strictly experimental equation (4) may become quite defective. Furthermore, it is valid only so long as the flanging does not touch the sheet border

$$D < b \tag{5a}$$

and the flanging does not overlap:

$$D < a_o = 0.8\ (D + 86)\sqrt{s}.$$

whence

$$D < \frac{86\sqrt{s}}{1.25 - \sqrt{s}} \tag{5b}$$

The last equation (5b) expresses the selection of D, especially for thin sheet. If it is not complied with the best value for the buckling load in shear P_{ko} is not within the constructively possible range; the holes would be greater than the spacing; the flangings would run into each other. For the thinnest sheet examined, $s = 0.4$ mm,

it is necessary that $D < \dfrac{86\sqrt{0.4}}{1.25 - \sqrt{0.4}}$ or $D < 88.5$ mm

according to equation (5b), while the diameter of the greatest flanges was only $D = 82$.

TABLE II

D mm	s mm	a_o mm	$\sqrt{s}$	$a = \frac{a_o}{\sqrt{s}}$	
62	0.42	76	0.648	117.5	
	.52	85	.721	118	$\alpha = 118$
	.615	93	.784	118.5	
	.8	100?	.894	112?	
72	0.52	90	0.721	125	$\alpha = 125$
	.8	> 89	.894	> 99.5	
82	0.42	89	0.648	137.5	
	.52	97	.721	134.5	$\alpha = 135$
	.615	{100 {110.5	.784	{127.5 {141	
	.8	> 106.5	.894	> 119	

BUCKLING LOAD IN SHEAR P_{ko} AND ITS PERTINENT a_o

When stressing sheets of the examined kind in shear the best hole spacing a_o (equation 4) must be adhered to if at all possible, to assure high loading without buckling. With this in mind, we did not determine P_{ko} for any hole spacing a, but rather the optimum P_{ko} for each pair of sheets of $L = 1.192$ mm with optimum hole spacing $a = a_o$.

For equal $b = 110$ mm and equal $D = 62$, $D = 72$, and $D = 82$, the $P_{ko} = f(s)$ values lie on three straight lines which intersect in a point with the coordinate $s = 0.54$ mm $P_{ko} = 1,700$ kg (fig. 14). This intersection point shall be the common point of all $P_{ko} = f(s)$ curves for $D =$ constant and $b = 110$ mm. For $s = 0.54$ mm the size of D is accordingly immaterial. In all sheets of 0.54 mm thickness, P_{ko} is the same, provided $a = a_o$. For

$$s < 0.54 \text{ mm}, \quad D \text{ must be small}, \tag{6a}$$

$$s > 0.54 \text{ mm}, \quad D \text{ must be great}. \tag{6b}$$

For thicker, inherently stiff sheets, the flangings must be equally stiff; that is, be of a certain depth which, in turn, is contingent upon large diameters.

The straight lines through the point [$s = 0.54$ mm, $P_{ko} = 1,700$ kg] may be expressed with

$$P_{ko} = 1700 + \beta\,(s - 0.54),$$

wherein β depends on D. According to figure 15, it is proportional to D. With $\beta = 95.6$ D, the optimum P_{ko} for sheet of $b = 110$ mm is:

$$P_{ko} = 1700 + 95.6\,D\,(s - 0.54).$$

The effect of b on P_{ko} was not thoroughly explored because a few cursory tests proved it to be quite subordinate while on the other hand, an exact elucidation of the effect of b would have entailed a very great number of further experiments. The small effect of b is due to the fact that the middle strip, weakened by holes, is above all decisive for the buckling, while the flat-edge strips are but little effective. It is therefore justified to assume that for sheets of different width the behavior relative to the individual quantities is substantially the same.

To allow for b the values obtained for $b = 110$ mm were given a correction factor dependent only on b and $= 1$ for $b = 110$ mm, while

for $b < 110$ mm, it must be > 1,

" $b > 110$ " " " " < 1,

because a narrow sheet does not buckle as easily as a wide one (equation 2). The correction factor f is tabulated in table III and plotted in figure 16.

TABLE III

D	s	a_o	p_{ko}				
			b=70	b=90	b=110	b=175	b=215
mm	mm	mm	mm	mm	mm	mm	mm
62	0.42	76	1260		1130		
	.52	85	1720	1600	1530		
	.615	92.5			2220	1500	
	.8	104			3040		
72	0.42	81.3			900		
	.52	90.7			1520		
	.8	111.5			3200		
					4000		
82	0.42	86.3			760		
	.52	96.5			1600	(1000)	1400
							1500
	.615	105				1700	
	.82	118.5			3720	(1700)	

It is seen that the obtained values may be closely approximated with a hyperbola of the form of

$$f = \alpha + \frac{\beta}{b}$$

To define α and β this formula is written as

$$f\,b = \alpha\,b + \beta,$$

a linear equation for $f\,b$ in terms of b. The straight line is also shown in figure 16. It gives:

$$\alpha = 0.767$$

$$\beta = 25.6$$

whence

$$f = \alpha + \frac{\beta}{b} = 0.767 + \frac{25.6}{b} = 25.6 \left(0.03 + \frac{1}{b}\right)$$

As the value for any b is to be f times as high as the P_{ko} value for $b = 110$ mm, we find for any width b

$$P_{ko} = 25.6 \left(0.03 + \frac{1}{b}\right) [1700 + 95.6\ D\ (s - 0.54)]$$

This value applies to a pair of sheets of $L = 1192$ mm. The buckling load in shear p_{ko} being, according to figure 12, proportional to L, it is for $L = 1$ mm, according to (3c):

$$p_{ko} = \frac{P_{ko}}{2\ L} = \frac{P_{ko}}{2 \times 1192} = \frac{P_{ko}}{2384}.$$

This formula, written in the preceding equation, gives the optimum p_{ko} value:

$$p_{ko} = \frac{25.6 \times 95.6}{2384} \left(0.03 + \frac{1}{b}\right) \left[\frac{1700}{95.6} + D\ (s - 0.54)\right]$$

For sheet with Young's modulus E not abnormally at variance with $E = 7{,}500$ kg/mm², the obtained p_{ko} value for $E = 7{,}500$ kg/mm² must be multiplied by the correction factor $E/7500$:

$$p_{ko} = \frac{E}{7500} \times 1.03 \left(0.03 + \frac{1}{b}\right) [17.8 + D\ (s - 0.54)]$$

$$p_{ko} = 1.36 \times 10^{-4}\ E \left(0.03 + \frac{1}{b}\right) [17.8 + D\ (s - 0.54)] \qquad (7)$$

This is on the premise that the buckling load in shear p_{ko} given in (7) is reached in kg/mm sheet length; that (4) is complied with, or in other words, that the optimum hole spacing $a = a_o$ has been chosen. As equation (4), so can (7) become very defective outside of the range investigated; i.e., outside of $D = 62$ to 82, $s = 0.4$ to 0.8 mm, $b = 75$ to 215 mm, because the formula merely represents an approximation formula from the obtained experimental values.

To show the accord of the optimum values of (7) with the experimental results, we computed $P_{ko} = 2 L p_{ko}$ with (3c) and (7), and included it in table I, together with the pertinent a_o value.

Admittedly, in airplane design a simple sheet shall never be so highly stressed as still allowed according to (7). Buckling generally occurs under lower shear stresses for various reasons. One thing is certain, however, and that is that it would serve no useful purpose to determine p_{ko} more accurately than in the present experiments, because actual buckling occurs quite frequently at loads which are from 20 to 40 percent lower than the theoretical p_{ko} value.

RELATIVE DISPLACEMENT δ_1

Lastly, we determine the displacement of the nonbuckled sheet. The shearing force P and the displacement v give the displacement of the sheets per 1 kg of tension at $\delta_L = v/P$, or with the values at buckling, P_k and v_k (table I), $\delta_L = v_k/P_k$. For sheets of length $L \cong 1192$ mm (standard length), the subscript L is omitted on δ_L. For these, we have:

$$\delta = \frac{v_k}{P_k}\left[\frac{mm}{kg}\right], \quad \text{and} \quad \delta = 10^6\frac{v_k}{P_k}\left[\frac{\mu}{t}\right].$$

The effect of flanging depth, which may be varied as known, by means of the hole diameter d (fig. 6), is subordinate. In a sheet having the dimensions:

$$L = 1{,}690 \text{ mm}, \quad b = 110 \text{ mm}, \quad s = 0.515 \text{ mm}$$

$$D = 72 \text{ "} \quad a = 90 \text{ "} \quad r = 80 \text{ "}$$

(sheets 43 to 45), δ_L ranged between 127 and 133 mm when d rose from 62.5 to 65.45 and the flanging depth $\sim 0.5\ (D - d)$ dropped from ~ 4.9 to ~ 3.275 mm.

The explanation for this minor effect is that the flanged hole compared to the full sheet is easily deformable in direction of the plane of the sheet. (Note the weakness of the flanged hole compared to the sheet, in fig. 9.) The displacement is almost exclusively governed by the flat portion of the sheet.

Since the displacement v of a smooth sheet is inversely proportional to the thickness s, namely, $v = \frac{P\ b}{G\ L\ s}$ (equation 1), δ also must be inversely proportional to s for smooth, full (unweakened) sheets. But according to the tests on sheets with flanged holes δ was not inversely proportional to s but needed, in addition, an exponent β:

$$\delta = \frac{\alpha}{s^{\beta}}.$$

Plotted in logarithmic coordinates (fig. 17), we have $\beta = 1.2$ for each investigated b, D, and a, with α, of course, depending upon these three quantities. To determine α we multiplied the obtained δ values with s^{β}:

$$\alpha = \delta\ s^{\beta} = \delta\ s^{1.2}.$$

For the determination of the influence of a on α, the space between the flanging $(a - D)$ is of prime importance. The greater the effective inter-space, the less is the displacement. The supposedly inverse proportionality $(a - D)$ fails to materialize; on the contrary $(a - D)$ must be augmented by an exponent γ:

$$\alpha = \frac{\epsilon}{(a - D)^{\gamma}}$$

The logarithmic graph (fig. 18) gives $\gamma = 0.75$; ϵ is as yet dependent on b and D. It may be defined from

$$\epsilon = \alpha\ (a - D)^{\gamma} = \alpha\ (a - D)^{0.75}$$

According to figure 19, ϵ rises linearly with b. With the intersection of the straight lines for $D = 62$ and $D = 82$, and the coordinates $b = 310$ mm and $\epsilon = 1230$ as the common intersection point of all straight lines $D =$ constant, the equations for ϵ become

$$\epsilon = 1230 - \lambda\ (310 - b)$$

with only λ dependent on D.

The linear course of $\epsilon = f\ (b)$ and thereby of $\delta = f\ (b)$ is due to the fact that for identical load the middle strip on otherwise identical sheets of different widths suffers approximately the same deformation and that the two flat-edge strips are augmented by a displacement proportional to the width of these edge strips. Logically, the whole displacement then increases in linear relation with b.

From the slope λ of the straight line ϵ in figure 19, we assume it to change linearly with respect to D. Then figure 20 gives $\lambda = 8.35 - 0.081\ D$.

The insertion of the obtained values α, β, γ, ϵ, and λ yields:

$$\delta = \frac{1230 - (310 - b)\ (8.35 - 0.081\ D)}{(a - D)^{0.75}\ s^{1.2}}\ .$$

Loading the sheets in 1 kg/mm of sheet length over $2L = 2 \times 1192 = 2384$ mm instead of in 1 kg gives the relative displacement δ_1, which is 2L times as high as δ. $\delta_1 = 2L\ \delta = 2384\ \delta$, when δ is measured in mm/kg, and

$$\delta_1 = 2384 \times 10^{-6}\ \delta$$

when δ is measured in $\frac{\mu}{t}$ and δ_1 in mm $\frac{mm}{kg}$. The final result then is:

$$\delta_1 = 2384 \times 10^{-6} \times 0.081 \times \frac{\frac{1230}{0.081} - (310 - b)\left(\frac{8.35}{0.081} - D\right)}{a - D^{0.75}\ s^{1.2}}$$

$$\delta_1 = 1.89 \times 10^{-4} \times \frac{15200 - (310 - b)\ (103 - D)}{(a - D)^{0.75}\ s^{1.2}} \qquad (8)$$

To prove the agreement between the values obtained from (8) and the experimental data, table I shows the obtained δ_1 values together with the computed value. Equation (8) is based upon strictly experimental findings, hence its validity is assured for only the range investigated.

COMPARISON WITH FULL SHEETS (NO HOLES) AND SHEETS WITH HOLES BUT NO FLANGING

In order to determine the suitability of flanged or plain holes as well as any eventual benefit accruing from such flanging, we investigated a sheet with and without flanged holes (table I, sheet No. 73). The nonflanged sheet collapsed under a shearing force of $P_k = 720$ kg; the corresponding displacement amounted to $\delta = 34\ \mu/t$. With flanged edge of $D = 52$ the buckling load rose to 1,240 kg, or 72 percent. Admittedly, δ likewise rose to $45\ \frac{\mu}{t}$, that is, 32.5 percent. With still greater holes but otherwise identical sheets: $d = 62.2$ (table I, sheet No. 45) which, without flanging, must naturally have still lower buckling values than sheet No. 73, a buckling load of $P_k = 2,300$ kg was obtained; of course, $\delta = 130\ \frac{\mu}{t}$, that is, markedly higher. This should be a definite proof of the value of flanging to raise the buckling load in shear. The greater relative displacement δ of the flanged versus the unflanged sheet is due to the fact that the flat portion, which after all takes up the greater part of the shearing forces, becomes smaller because of the flanging.

Lastly, we investigated several full sheets (without holes) and compared the obtained buckling load with Southwell and Skan's data (reference 6). The agreement is close according to table I, sheets Nos. 74 to 78. The conclusion that the accord between the theoretical and experimental values for flanged sheets is close, is therefore justified.

In order to determine whether and to what extent a flanged sheet is more resistant to buckling than a smooth, full sheet, we included in table I, aside from a_o (equation 4) and p_{ko} (equation 7) the p_{ku} value of the full sheet (equation 2). It was found that in particularly thin, wide sheets which without holes have a very low buckling load in shear p_{ku}, the stiffening influence of flanged holes results in a many times greater p_{ku}; while in thicker, narrower sheets, inherently very resistant to bending, the higher stress due to reduction in effective, flat surface, it results in weakening. Admittedly, it is necessary to decide in each individual case, whether stiffening or weakening occurs by a comparison of p_{ko} with p_{ku}.

REFERENCES

1. Bryan, G. H.: On the Stability of a Plate Under Thrusts in Its Own Plane, with Applications to the "Buckling" of the Sides of a Ship. Proc. of the London Math. Soc., vol. 22, 1891, p. 54.

2. Lilly, W. E.: Web Stresses in Plate Girders and Columns. Engineering, February 1, 1907, pp. 136-139.

3. Lilly, W. E.: The Design of Struts. Engineering, vol. 85, 1908, pp. 37-40.

4. Timoschenko, S.: Über die Stabilität versteifter Platten; Der Eisenbau, vol. 12, 1921, pp. 147-163.

5. Ritz, W.: Über eine Methode zur Lösung gewisser Variationsprobleme der mathematischen Physik. Journal f. d. reine und angew. Mathematik, vol. 135, p. 1. (See also his collected works, Paris, 1911.)

6. Southwell, R. V., and Skan, Sylvia W.: On the Stability Under Shearing Forces of a Flat Elastic Strip. Proc. Roy. Soc., series A, vol. 105.

7. Coker, E. G.: Optical Determination of the Variation of Stresses in a Thin Rectangular Plate Subjected to Shear. Proc. Roy. Soc., series A, vol. 86, 1911, pp. 291-319.

8. Bollenrath, Fr.: Ausbeulerscheinungen an ebenen, auf Schub beanspruchten Platten. Luftfahrtforschung, vol. 6, 1930, pp. 1-17.

9. Mathar, J.: Beitrag zur Schubsteifigkeit und Knickfestigkeit von gelochten dünnen Platten. Abhdlg. a. d. Aerodyn. Inst. d. Technical High School, Aachen, No. 10. 1931.

10. Seydel, E.: Beitrag zur Frage des Ausbeulens von versteiften Platten bei Schubbeanspruchung. Luftfahrtforschung, vol. 8, no. 3.

11. Schmieden, C.: Das Ausknicken versteifter Bleche unter Schubbeanspruchung. Z.F.M., vol. 21, 1930, p. 61.

12. Bergmann, S., and Reissner, H.: Über die Knickung von Wellblechstreifen bei Schubbeanspruchung. Z.F.M., Sept. 28, 1929, p. 475; and Z.F.M., vol. 21, 1930.

13. Jennissen, J.: Über Wellblech bei Schubbeanspruchung. Diss. Aachen, 1931. (Unpublished.)

14. Hirota, M.: Über den Spannungszustand in einem durchlochten Streifen. Diss. Aachen, 1931.

Translation by J. Vanier,
National Advisory Committee
for Aeronautics.

Table I

Sheet No.	s mm	a mm	d mm	L mm	P_k kg	v_k μ	p_k $\frac{kg}{mm}$	δ $\frac{\mu}{t}$	δ_1 $\frac{mm^2}{kg}$ Measured	Calculated
$D = 62$ mm, $b = 70$ mm										
1	0,52	71	~0,8 D	~1192	1500	295	0,63	197	0,465	0,431
2		76			1510	200	0,633	132	0,318	0,307
3		82			1630	155	0,685	95	0,227	0,233
		$a_0 = 86$					$p_{ko} = 0,758$			
							$p_{ku} = 1,672$			
4		89	51,3		1710	131	0,72	77	0,182	0,186
5			51		1730	129	0,73	75	0,175	
6	0,615	76	~0,8 D		1600	173	0,67	108	0,257	0,252
		$a_0 = 94$					$p_{ko} = 1,0$			
							$p_{ku} = 2,775$			
7	0,8	76			2500	197	1,05	79	0,188	0,183
8		89			1840	82	0,77	44,5	0,106	0,112
		$a_0 = 106$					$p_{ko} = 1,56$			
							$p_{ku} = 6,55$			
$D = 62$ mm, $b = 90$ mm										
9	0,52	76			1460	214	0,612	146	0,384	0,353
10		82			1500	171	0,63	114	0,272	0,268
		$a_0 = 86$					$p_{ko} = 0,665$			
							$p_{ku} = 1,042$			
11	0,615	76			1580	195	0,663	124	0,293	0,288
		$a_0 = 94$					$p_{ko} = 0,933$			
							$p_{ku} = 1,72$			
12	0,8	76	~0,8 D	~1192	2400	221	1,05	92	0,222	0,21
		$a_0 = 106$					$p_{ko} = 1,46$			
							$p_{ku} = 3,97$			
$D = 62$ mm, $b = 110$ mm										
13	0,42	71	~0,8 D	~1192	1080	380	0,435	352	0,840	0,725
14		76			1130	260	0,473	230	0,548	0,515
		$a_0 = 77$					$p_{ko} = 0,42$			
							$p_{ku} = 0,358$			
15		89			500	74	0,21	148	0,353	0,312
16	0,52	71			1440	340	0,604	236	0,56	0,558
17		71		765	930	330	0,608	355		
18		71		1690	2060	350	0,608	170		
19		76		~1192	1400	235	0,587	168	0,4	0,397
20		76			1410	241	0,592	171	0,408	0,397
21		82			1540	241	0,647	139	0,332	0,303
		$a_0 = 86$					$p_{ko} = 0,627$			
							$p_{ku} = 0,722$			
22		89			1520	155	0,638	102	0,243	0,24
23		89			1410	156	0,592	111	0,265	0,24
24		97			1280	110	0,537	86	0,205	0,198
25		106,5			1160	92	0,487	79	0,188	0,175
26		118			1325	91	0,555	69	0,164	0,136
27	0,615	76			1570	211	0,658	134	0,32	0,325
28		82			1900	205	0,797	108	0,258	0,248
29		89			2200	188	0,922	85,5	0,207	0,196
		$a_0 = 94$					$p_{ko} = 0,883$			
							$p_{ku} = 1,25$			
30		106,5			2200	150	0,922	68	0,162	0,14
31	0,8	71	~0,8 D	~1192	1600	226	0,67	141	0,336	0,333
32		76			2440	243	1,02	99,5	0,237	0,237
33		89			2900	185	1,22	64	0,152	0,143
34		97			3000	162	1,26	54	0,128	0,118
		$a_0 = 106$					$p_{ko} = 1,37$			
							$p_{ku} = 2,46$			
$D = 62$ mm, $b = 175$ mm										
35	0,615	71			1210	252	0,508	208	0,505	0,634
36		82			1500	184	0,63	123	0,293	0,343
		$a_0 = 86$					$p_{ko} = 0,805$			
							$p_{ku} = 0,444$			
$D = 72$ mm, $b = 110$ mm										
	0,42	$a_0 = 82$					$p_{ko} = 0,365$			
							$p_{ku} = 0,358$			
38		89			800	190	0,336	237	0,573	0,57
39	0,52	76			1200	660	0,503	550	1,31	1,32
40		85		1690	2220	364	0,658	164	0,533	0,542
41		89		~1192	1500	275	0,63	184	0,435	0,44
42		90		790	1090	292	0,688	268	0,457	0,42
43		90	60,2	1690	2280	300	0,675	132	0,446	0,42
44		90	56,2	1690	2300	293	0,68	128	0,43	0,42
45		90	62,25	1690	2300	298	0,68	130	0,44	0,42
		$a_0 = 91$	~0,8 D				$p_{ko} = 0,66$			
							$p_{ku} = 0,722$			
46		102		1690	2000	176	0,592	88	0,304	0,285
47		118		1690	1400	94	0,413	67	0,243	0,206
48	0,8	76	~0,8 D	~1192	1430	427	0,6	298	0,76	0,785
49		89			3210	374	1,35	116	0,278	0,262
		$a_0 = 99$					$p_{ko} = 1,47$			
							$p_{ku} = 2,46$			
$D = 82$ mm, $b = 90$ mm										
50	0,615	89			1500	540	0,63	361	0,845	0,832
51		97			1610	347	0,675	215	0,513	0,467
		$a_0 = 106$					$p_{ko} = 0,69$			
							$p_{ku} = 1,72$			
52		106,5			1600	197	0,671	123	0,398	0,322
$D = 82$ mm, $b = 110$ mm										
	0,42	$a_0 = 87$					$p_{ko} = 0,32$			
							$p_{ku} = 0,358$			
54		89			540	325	0,227	602	1,45	1,37
55		97			560	213	0,272	328	0,78	0,768
56		106,5			580	134	0,243	231	0,56	0,527
57	0,52	89			1290	630	0,542	490	1,18	1,06
58		90		1690	1900	580	0,562	305	1,05	0,96
59		97		~1192	1600	401	0,67	251	0,592	0,595
		$a_0 = 97$					$p_{ko} = 0,652$			
							$p_{ku} = 0,722$			
60		106,5			1300	217	0,545	166	0,398	0,407
61		118			1180	152	0,495	129	0,312	0,305
62	0,615	89			1170	460	0,491	393	0,945	0,87
		$a_0 = 106$					$p_{ko} = 0,933$			
							$p_{ku} = 1,25$			
63	0,8	89	~0,8 D	~1192	1400	382	0,587	272	0,658	0,632
64		97			2580	390	1,08	151	0,36	0,354
65		118			3700	290	1,55	78	0,191	0,182
		$a_0 = 120$					$p_{ko} = 1,58$			
							$p_{ku} = 2,46$			
$D = 82$ mm, $b = 175$ mm										
66	0,52	89			800	375	0,336	470	1,12	1,24
		$a_0 = 97$					$p_{ko} = 0,6$			
							$p_{ku} = 0,276$			
67		106,5			970	204	0,407	210	0,502	0,476
68	0,615	97			1450	331	0,608	228	0,548	0,57
		$a_0 = 106$					$p_{ko} = 0,85$			
							$p_{ku} = 0,44$			
69	0,8	89			1270	390	0,533	307	0,76	0,736
70		97			1370	234	0,575	170	0,41	0,414
		$a_0 = 120$					$p_{ko} = 1,44$			
							$p_{ku} = 0,94$			
$D = 82$ mm, $b = 215$ mm										
71	0,52	89			675	350	0,283	518	1,24	1,27
		$a_0 = 97$					$p_{ko} = 0,575$			
							$p_{ku} = 0,178$			
72		106,5			1400	292	0,587	208	0,495	0,492
$D = 82$ mm, $b = 110$ mm, not flanged										
73	0,55	90		1690	720	24	0,302	34	0,115	
73*)					1240	56	0,52	45	0,152	0,128
		$a_0 = 82$				56	$p_{ko} = 0,72$			
$D = 82$ mm, $b = 110$ mm, no holes										
74	0,42			1192	860	40	0,397	46,5	0,105	0,091
							err. 0,358			
75	0,525				1500	55	0,69	36,5	0,079	0,073
							err. 0,722			
76	0,525				1600	56	0,737	35	0,076	0,073
							err. 0,722			
77	0,615			1158	2180	62	1,01	28,5	0,0623	0,0615
							err. 1,25			
78	0,815			1192	6050	137	2,78	22,5	0,049	0,0464
							err. 2,61			

*) Sheet 73 flanged to $D = 52$ mm

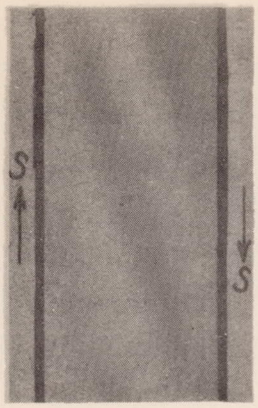

Figure 1.- Buckling in shear on a flat sheet.

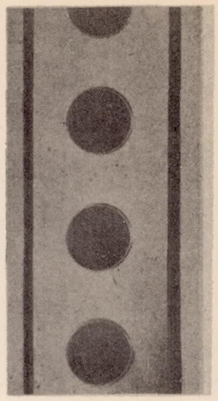

Figure 3.- Flanged sheet.

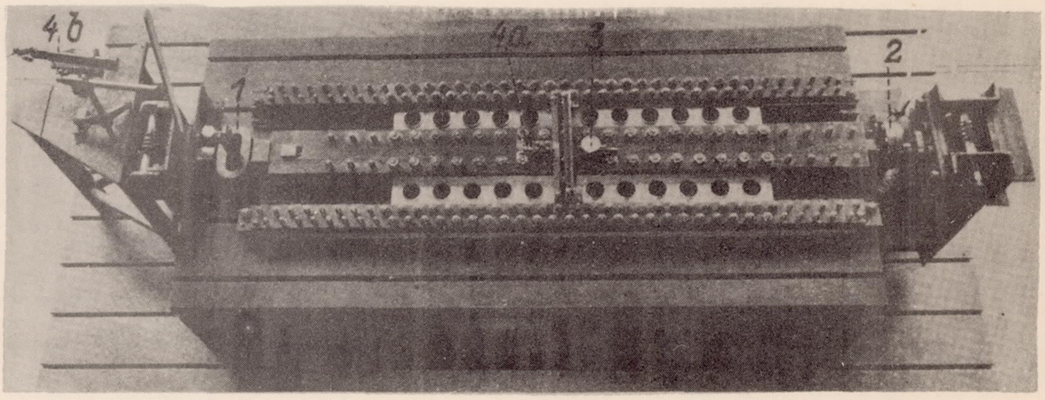

Figure 2.-Experimental setup.

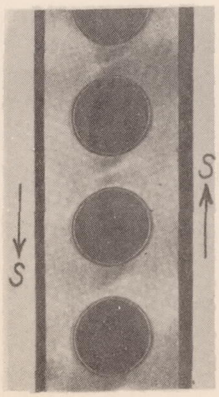

Figure 5.- Buckling in shear on a flanged sheet.

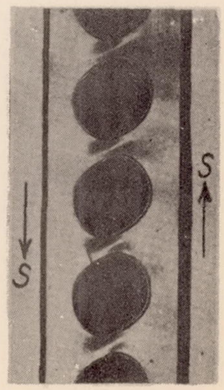

Figure 9.- Sheet distorted in shear showing torn flanging.

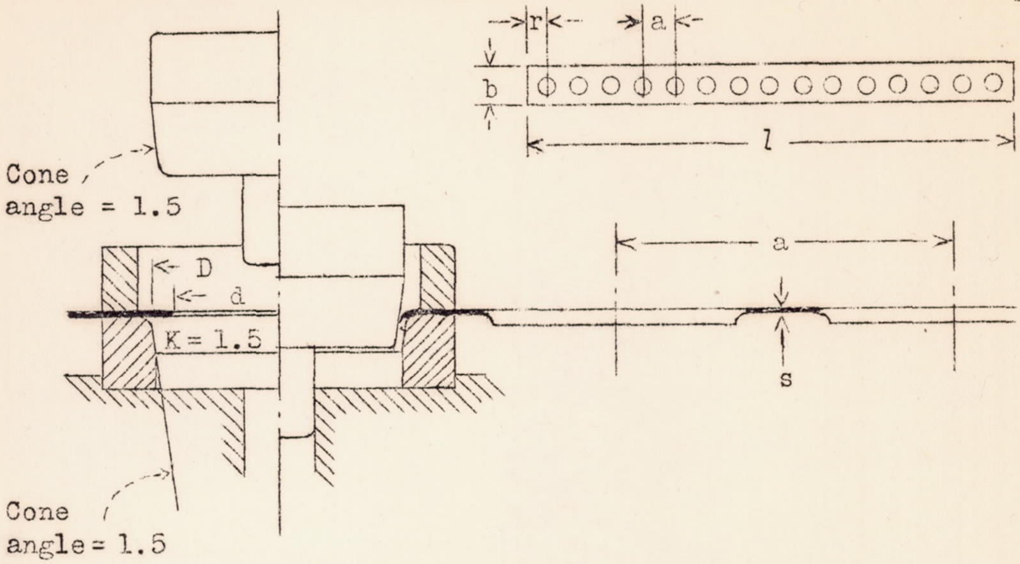

Figure 4.- Flanged sheet and flanging equipment.

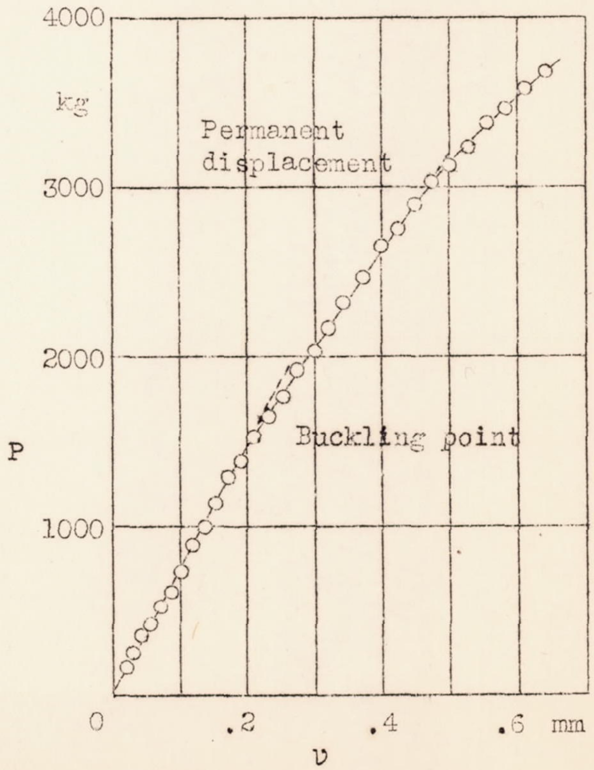

Figure 6.- Shearing force-displacement diagram.

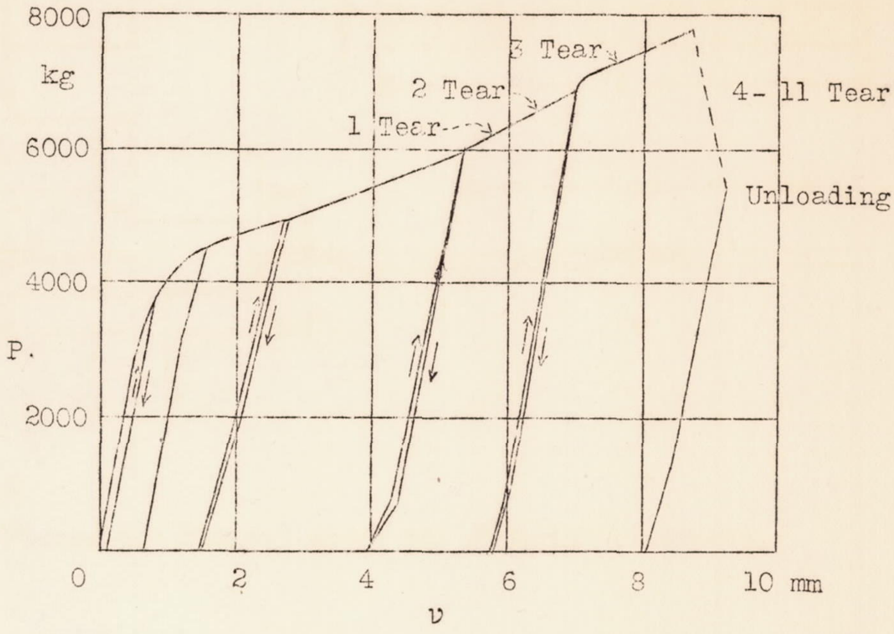

Figure 7.- Shearing force-displacement diagram with great displacements.

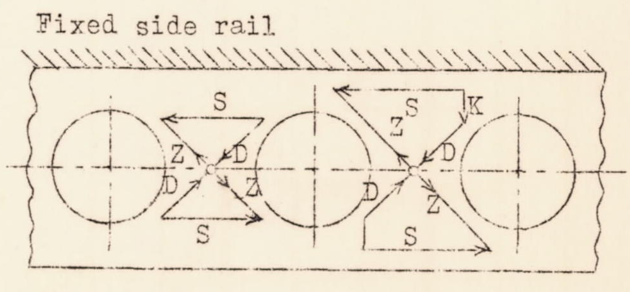

Figure 8.- Distribution of shearing force before and after buckling.

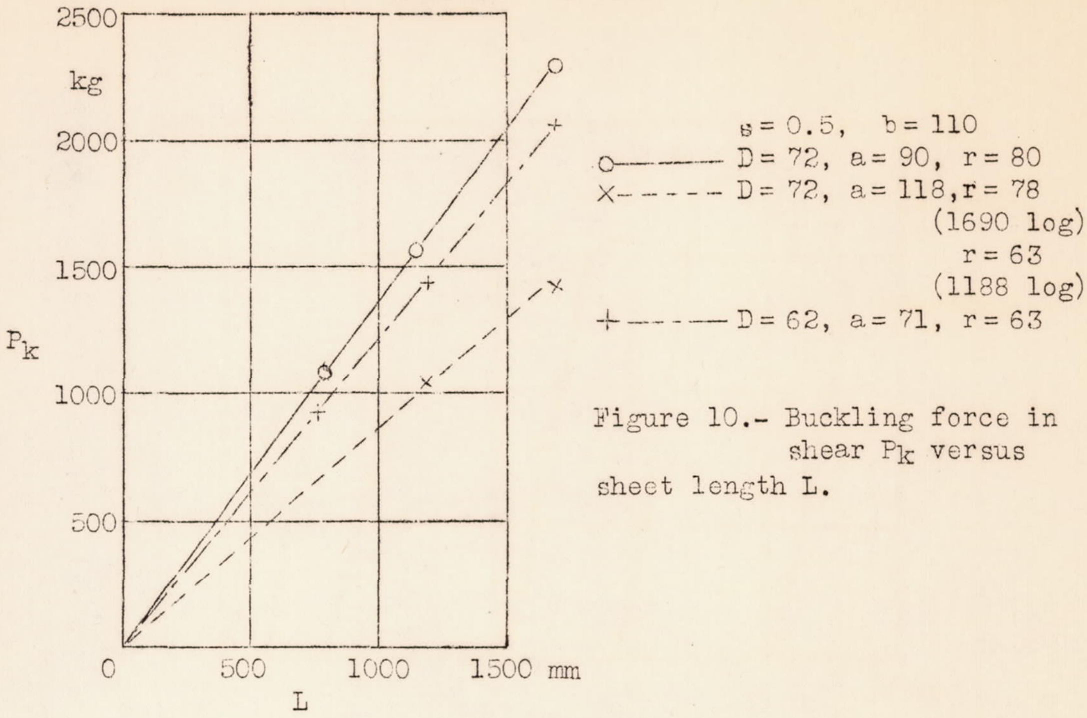

Figure 10.- Buckling force in shear P_k versus sheet length L.

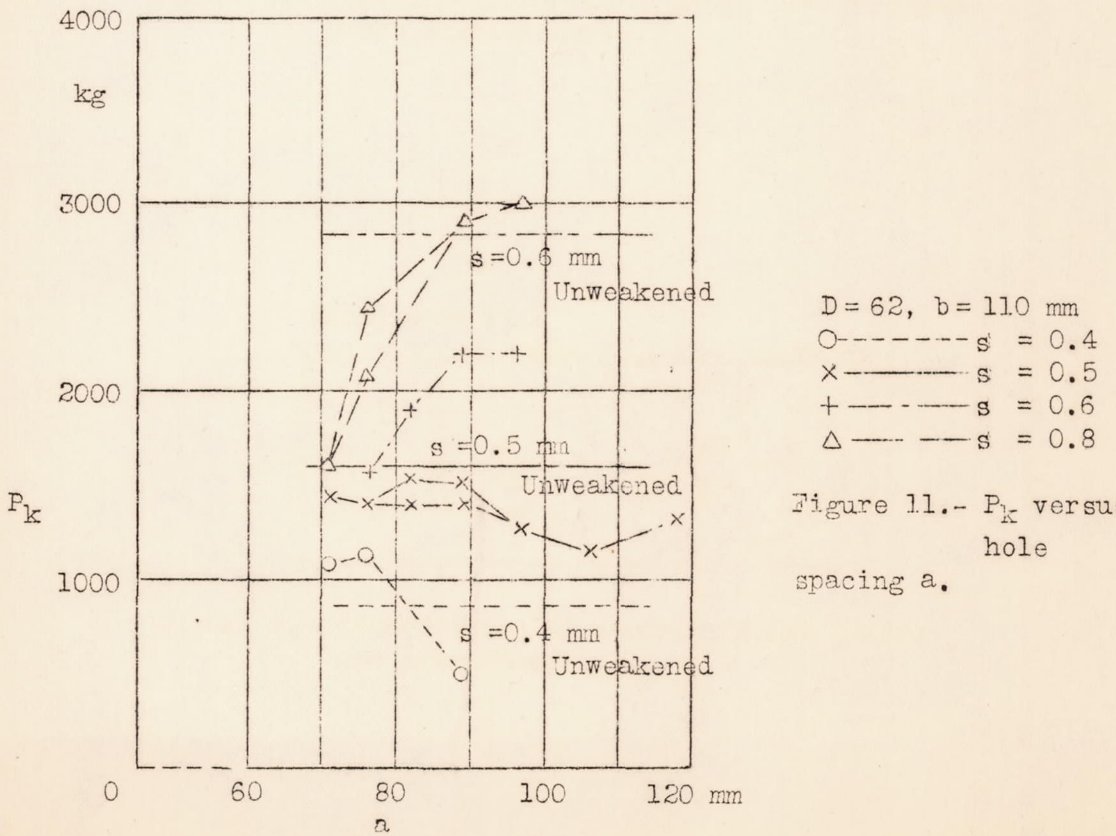

Figure 11.- P_k versus hole spacing a.

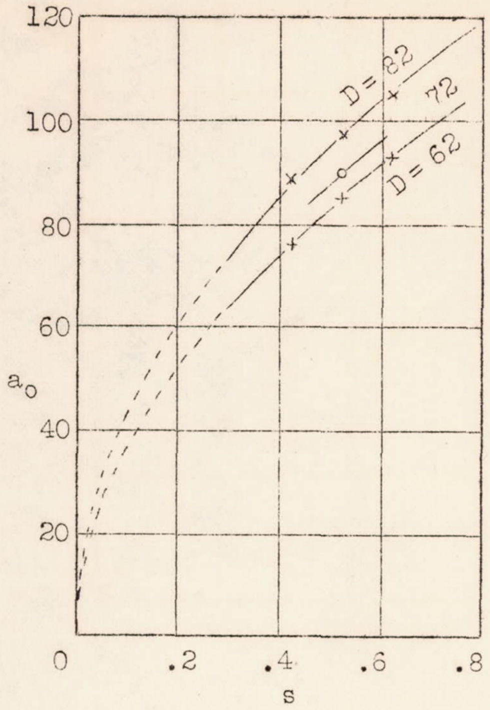

Figure 12.- Optimum hole spacing a_o versus sheet thickness s.

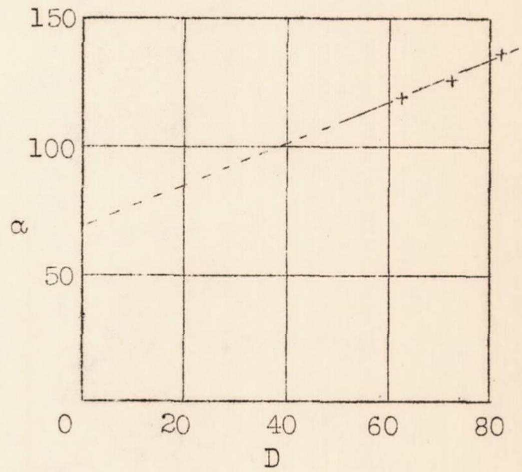

Figure 13.- Factor α versus D.

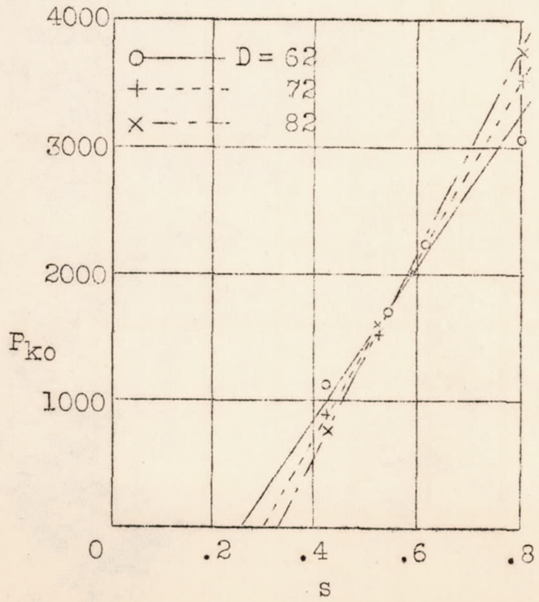

Figure 14.- Optimum P_{ko} versus s

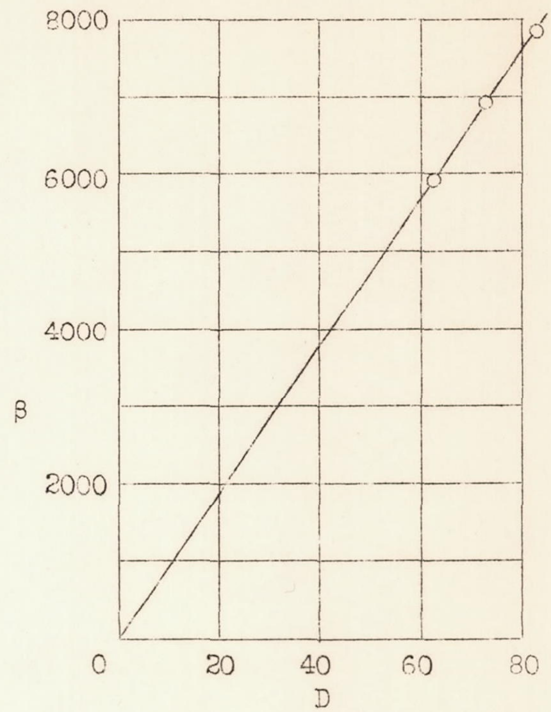

Figure 15.- Factor β versus D

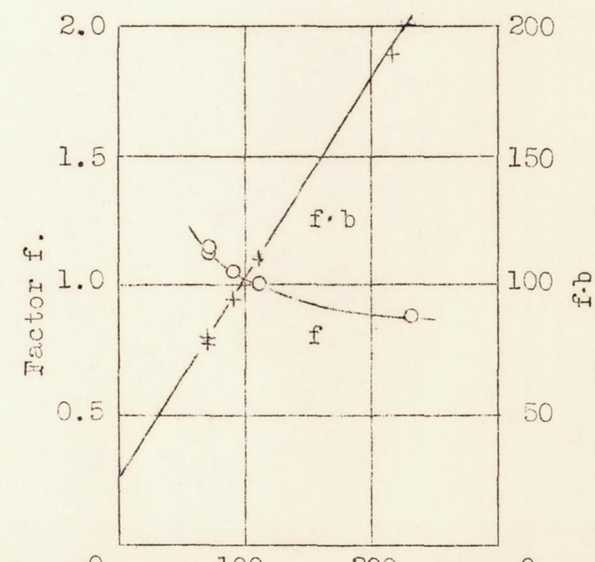

Figure 16.- Correction factor f versus b.

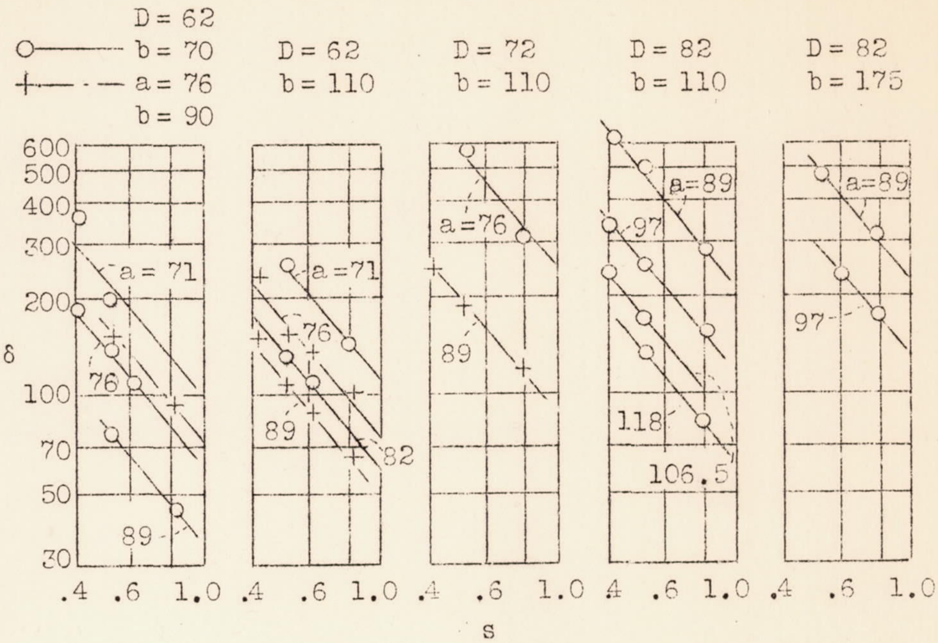

Figure 17.- Displacement δ for 1 kg shearing force versus s (log scale).

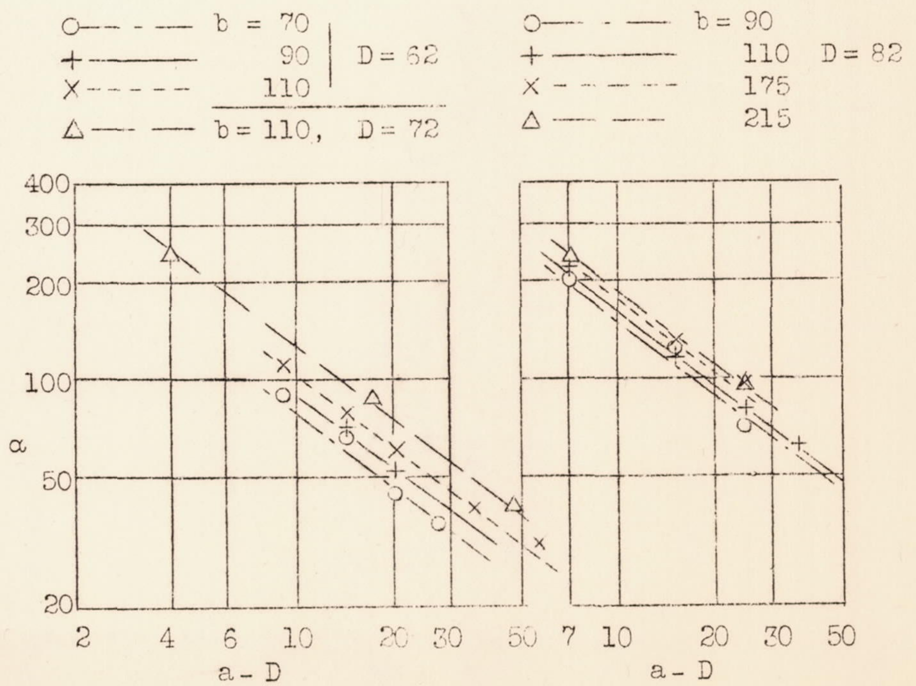

Figure 18.- Coefficient α versus space (a - D) between flangings.

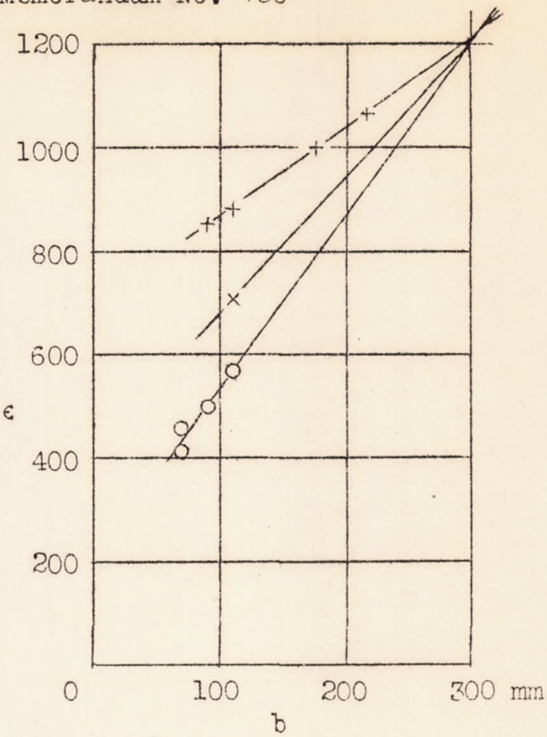

Figure 19.- Factor ε versus b.

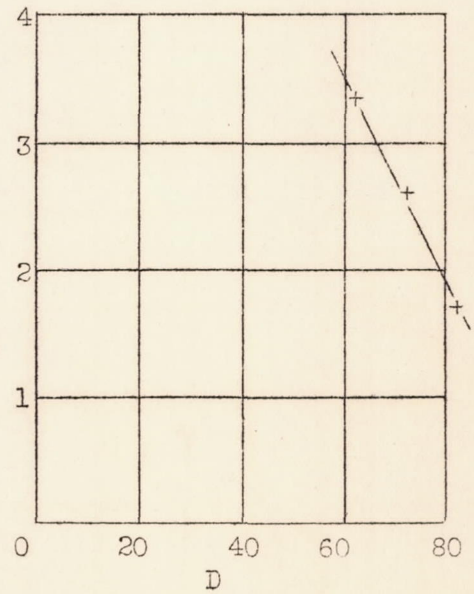

Figure 20.- Slope λ of straight line of figure 19 versus D.